

**Correlation between elliptic flow and shear viscosity in intermediate-energy heavy-ion collisions**C. L. Zhou (周铨龙),<sup>1</sup> Y. G. Ma (马余刚),<sup>1,2,\*</sup> D. Q. Fang (方德清),<sup>1</sup> G. Q. Zhang (张国强),<sup>1</sup> J. Xu (徐骏),<sup>1</sup>  
X. G. Cao (曹喜光),<sup>1</sup> and W. Q. Shen (沈文庆)<sup>1,2</sup><sup>1</sup>*Shanghai Institute of Applied Physics, Chinese Academy of Sciences, Shanghai 201800, China*<sup>2</sup>*Shanghai Tech University, Shanghai 200031, China*

(Received 2 August 2014; published 18 November 2014)

The correlation between the elliptic flow  $v_2$  scaled by the impact parameter  $b$  and the shear viscosity  $\eta$  as well as the specific viscosity  $\eta/s$ , defined as the ratio of the shear viscosity to the entropy density  $s$ , is investigated for the first time in intermediate-energy heavy-ion collisions based on an isospin-dependent quantum molecular dynamic model. The elliptic flow is calculated at balance energies to exclude the geometric influence such as the blocking effect from the spectators. Our study shows that  $v_2/b$  decreases almost linearly with increasing  $\eta$ , consistent with that observed in ultrarelativistic heavy-ion collisions. On the other hand,  $v_2/b$  is found to increase with increasing  $\eta/s$ .

DOI: [10.1103/PhysRevC.90.057601](https://doi.org/10.1103/PhysRevC.90.057601)

PACS number(s): 25.70.-z, 21.65.Mn

One of the most important points in heavy-ion collisions is the phase transition of strongly interacting matter, e.g., the transition between quark-gluon plasma (QGP) and hadronic matter at ultrarelativistic energies, as well as the liquid-gas phase transition at intermediate energies [1–13]. Recently, one interesting probe of the phase transition is the so-called specific viscosity  $\eta/s$ , defined as the ratio of the shear viscosity  $\eta$  to the entropy density  $s$ . Empirical observations of the temperature or incident energy dependence of  $\eta/s$  for H<sub>2</sub>O, He, and Ne<sub>2</sub> show a minimum in the vicinity of the phase transition temperature [14]. In addition, with increasing temperature, it is found that  $\eta/s$  decreases steeply below and rises slowly above the critical temperature for a wide class of systems. Nevertheless, a lower bound of  $\eta/s \geq 1/4\pi$ , obtained by Kovtun-Son-Starinets for infinitely coupled supersymmetric Yang-Mills gauge theory based on the AdS/CFT duality conjecture, is speculated to be universally valid [15]. It is thus very important to study  $\eta/s$  of strongly interacting matter created in heavy-ion collisions at both ultrarelativistic and intermediate energies.

The most common approach to the study of the transport properties of QGP formed in ultrarelativistic heavy-ion collisions is to investigate the effects of  $\eta/s$  on the elliptic flow in a viscous hydrodynamic model [16–18]. This approach has been implemented to simulate heavy-ion collisions at the Relativistic Heavy-Ion Collider and Large Hadron Collider, and it works well in midcentral collisions or at higher energies. In peripheral collisions or at lower energies, however, the hydrodynamic model should be followed by a microscopic transport simulation for the highly dissipative hadronic phase [19,20]. In addition, the hydrodynamics failed to describe the intermediate-energy heavy-ion collisions, which evolve mainly in hadronic degrees of freedom. Therefore, no efforts have been devoted to studying the viscous effect on elliptic flow in intermediate-energy heavy-ion collisions. However, some transport models [8–11], e.g., the isospin-dependent quantum molecular dynamic (IQMD) model and the Boltzmann-Uehling-Uhlenbeck (BUU) model, as well as

an isospin- and momentum-dependent interaction [12,13], can give very reasonable results for intermediate-energy heavy-ion collisions. In our previous studies, efforts were made to study the liquid-gas phase transition through  $\eta/s$  based on the IQMD and BUU models, and a good agreement with previous analyses was found.

It is worth mentioning that the dynamic evolution is more complex in low- and intermediate-energy heavy-ion collisions. For instance, the elliptic flow at low energies is related to the rotation of the compound system with the expansion of the hot and compressed participant zone and possibly modified by the shadowing effect of the cold spectator matter. In heavy-ion collisions at ultrarelativistic energies, however, the spectators are quickly separated from the participants, and the participant portion can evolve without the influence of the spectator matter. It is thus seen that the elliptic flow is positive at low energies, becomes negative at intermediate energies, and is positive again at relativistic energies [21–23]. In transport model simulations for intermediate-energy heavy-ion collisions, nucleon interactions are described by mean fields as well as nucleon-nucleon (N-N) scatterings in the whole reaction process. With increasing collision energy, N-N scatterings become dominant for the dynamics and are responsible for the deflection of hot compressed participant matter from cold spectator matter, while the attractive portion of the mean field becomes more important with decreasing collision energy. These observations indicate that the collective flow of the participant portion mainly suffers the compression and pulling-out effects from the spectator matter. Therefore, the viscous effect shall be studied once the influence of the spectator on the elliptic flow has been successfully removed.

Fortunately, the two competing effects of mean fields and N-N scatterings largely balance each other at the so-called balance energy, characterized by a vanishing directed flow [24–27], i.e., when the slope parameter  $F_d$  of the directed flow denoting the average transverse momentum in the reaction plane at midrapidity becomes 0. The influence of the spectator matter on the participant matter is relatively small in collisions at the balance energy, and these collisions provide an excellent opportunity to study the viscous effect on the elliptic flow. One

\*Corresponding author: [ygma@sinap.ac.cn](mailto:ygma@sinap.ac.cn)

should keep in mind that the referred balance between mean fields and N-N collisions does not mean that they are balanced during the whole collision process. At the maximum compressed stage the N-N scatterings are stronger, while the mean fields take over after some time of expansion. This means that the participant portion is still influenced by the spectator matter in the expansion stage. It is thus difficult to calculate reasonably the conventional spatial-eccentricity-scaled elliptic flow  $v_2/\epsilon$  [28,29], because the spatial eccentricity, which is defined as  $\epsilon = \langle y^2 - x^2 \rangle / \langle y^2 + x^2 \rangle$ , characterizing the anisotropy in the coordinate space, changes throughout the whole collision process. Differently from that in ultrarelativistic heavy-ion collisions, an impact-parameter-scaled elliptic flow  $v_2/b$  is introduced to eliminate the geometric effect in the present study.

Our study is based on an IQMD model [30–32]. In this framework, each nucleon is represented by a Gaussian wave packet in coordinate and momentum space to partially take into account quantum effects, and the equation of motion for the center of the wave packet evolves according to the classical equation of motion based on the Hamiltonian of the system from effective nucleon interactions. The effective mean field used in the IQMD model can be expressed as [31]

$$U = U_{\text{Sky}} + U_{\text{Coul}} + U_{\text{Yuk}} + U_{\text{sym}}, \quad (1)$$

where  $U_{\text{Sky}}$ ,  $U_{\text{Coul}}$ ,  $U_{\text{Yuk}}$ , and  $U_{\text{sym}}$  are the bulk Skyrme potential, the Coulomb potential, the surface Yukawa potential, and the isospin asymmetry potential, respectively. The bulk Skyrme potential is

$$U_{\text{Sky}} = \alpha(\rho/\rho_0) + \beta(\rho/\rho_0)^\gamma, \quad (2)$$

where  $\rho$  is the nucleon number density and  $\rho_0 = 0.16 \text{ fm}^{-3}$  is the saturation density. In this work, the parameters  $\alpha = -356 \text{ MeV}$ ,  $\beta = 303 \text{ MeV}$ , and  $\gamma = 7/6$ , corresponding to a soft equation of state, are used. The expressions of the other potentials can be found in our previous work [8,9]. Within the present framework, reasonable phase-space information on nucleons and fragments in intermediate-energy heavy-ion collisions is obtained. About 50 000  $^{197}\text{Au} + ^{197}\text{Au}$  collision events have been simulated using the IQMD model for different impact parameters and beam energies for the investigation of the correlation between the elliptic flow and the shear viscosity in the present study.

The slope parameter of the directed flow in noncentral heavy-ion collisions can be expressed as

$$F_d = \frac{d\langle p_x/A \rangle}{d(y/y_b)}, \quad (3)$$

where  $p_x$  is the projection of the transverse momentum in the reaction plane,  $A$  is the number of nucleons, and  $y/y_b$  is the particle rapidity  $y$  normalized by the beam rapidity  $y_b$ . The extracted  $F_d$  from the IQMD model versus the impact parameter  $b$  at different beam energies is shown in Fig. 1. The dashed line in  $F_d = 0$  is plotted as a guide for the eye. With an increase in the impact parameter, it is seen that the  $|F_d|$  generally increases, passes through a maximum value, and diminishes in most peripheral collisions [33,34]. In addition,  $F_d$  is negative at the lower energy of 40 MeV/u, positive at the higher energies of 55–60 MeV/u, and 0 around 45–50 MeV/u, consistent with the findings in Refs. [35–38]. The

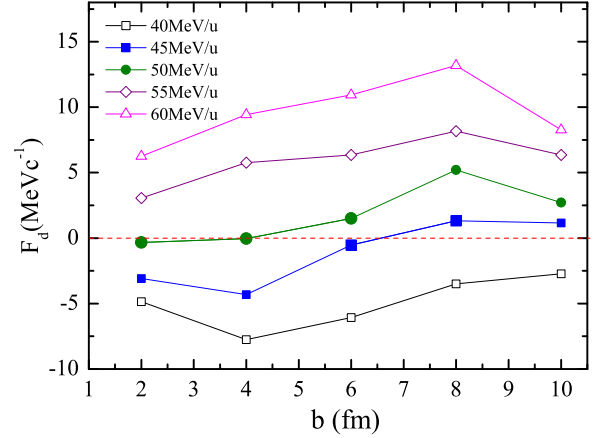


FIG. 1. (Color online) The extracted slope parameter  $F_d$  of the directed flow as a function of the impact parameter  $b$  in heavy-ion collisions at different beam energies.

collision energies and impact parameters with  $F_d$  closest to 0 are [50 MeV/u, 2 fm], [50 MeV/u, 4 fm], [50 MeV/u, 6 fm], [45 MeV/u, 6 fm], and [45 MeV/u, 8 fm], respectively. In these collisions, the effects from the mean field and N-N scatterings cancel each other so that the influence of the blocking from the spectator matter on the elliptic flow could be negligible.

For largely equilibrated systems, fluxes of macroscopic quantities are proportional to the field gradient of the system. The shear viscosity  $\eta$  is the coefficient of proportionality between the shear force between flow layers per unit area, i.e., the momentum flux, and the velocity gradient, and it can be understood from the fluctuation-dissipation theorem [39]. In the limit of Boltzmann statistics, the shear viscosity corresponds to the first-order Chapman-Enskog coefficient and can be expressed as a parameterized function by Danielewicz [40,41],

$$\eta\left(\frac{\rho}{\rho_0}, T\right) = \frac{1700}{T^2} \left(\frac{\rho}{\rho_0}\right)^2 + \frac{22}{1 + T^2 10^{-3}} \left(\frac{\rho}{\rho_0}\right)^{0.7} + \frac{5.8\sqrt{T}}{1 + 160T^{-2}}, \quad (4)$$

where the shear viscosity  $\eta$  and the temperature  $T$  are in  $\text{MeV}/\text{fm}^2c$  and  $\text{MeV}$ , respectively. The above equation is reliable if the system is locally equilibrated with density  $\rho$  and temperature  $T$ , with the former calculated from the overlap of the nucleon wave packets and the latter, as well as the entropy density  $s$ , obtained from the generalized Thomas-Fermi formalism at finite temperature [42–45]. The average shear viscosity  $\langle \eta \rangle$ , entropy density  $\langle s \rangle$ , and specific viscosity  $\langle \eta/s \rangle$  in the center of the system from the moment of maximum compression to freeze-out for the five selected beam energies and impact parameters are given in Figs. 2(a), 2(b), and 2(c), respectively. It is interesting to see that  $\langle \eta \rangle$  decreases with increasing impact parameter. This can be understood from the classical relation  $\eta \sim \langle p \rangle / \sigma$ , where the average momentum  $\langle p \rangle$  is higher in more central collisions while the N-N scattering cross section  $\sigma$  is the same. In addition,  $\langle s \rangle$  is also larger in more central collisions due to the higher temperature.

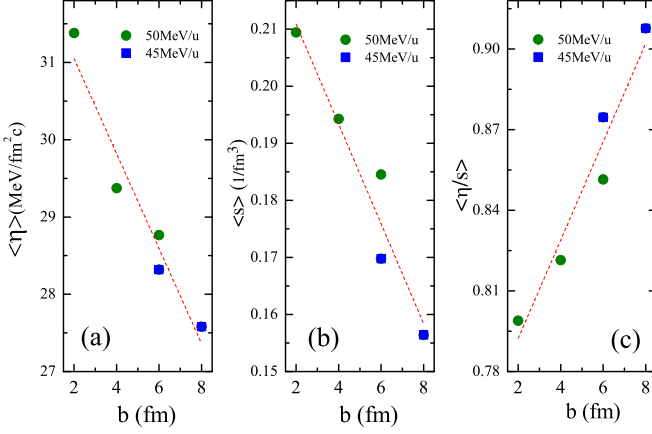


FIG. 2. (Color online) The extracted average shear viscosity (a), entropy density (b), and specific viscosity (c) at balance energies and corresponding impact parameters. Dashed lines are guides for the eye.

After taking the ratio, the average specific viscosity  $\langle\eta/s\rangle$  somehow increases with increasing impact parameter.

The elliptic flow is defined as the second-order harmonic coefficient of Fourier expansion of the particle azimuthal distribution,

$$v_2 = \langle \cos(2\phi) \rangle = \left\langle \frac{p_x^2 - p_y^2}{p_x^2 + p_y^2} \right\rangle, \quad (5)$$

where  $\phi$  is the azimuthal angle,  $p_x$  and  $p_y$  are the projections of the transverse momentum parallel and perpendicular to the reaction plane, respectively, and the angle brace denotes the average over all particles. The elliptic flow can be determined by the collective motion resulting from the rotation of the compound system, the expansion of hot and compressed participant matter, and the possible modification by the shadowing effect of cold spectator matter [46–51]. Similarly to the directed flow, generally the elliptic flow first increases with increasing impact parameter, then reaches a maximum in midcentral collisions, and, finally, decreases at large centralities. In this work emitted light fragments of charge number  $Z \leq 3$  including protons and neutrons at midrapidity  $|y/y_b| \leq 0.1$  are employed to calculate the elliptic flow at freeze-out. The impact parameter dependence of  $v_2$  and that scaled by the impact parameter are shown in Figs. 3(a) and 3(b), respectively. The positive value of  $v_2$  indicates that an in-plane emission of particles is observed at balance energies. It is shown in Fig. 3(a) that  $v_2$  increases linearly with increasing impact parameter, and the  $v_2$  at [45 MeV/u, 8 fm] is about 10 times that at [50 MeV/u, 2 fm]. After scaling by the impact parameter, this difference is reduced to about 2 times as shown in Fig. 3(b), and we argue that the remaining difference is due to the viscous effect in intermediate-energy heavy-ion collisions.

Combining Fig. 2 and Fig. 3, the correlations between  $v_2/b$  and  $\langle\eta\rangle$  as well as  $\langle\eta/s\rangle$  are exhibited in Figs. 4(a) and 4(b), respectively. It is found that  $v_2/b$  decreases almost linearly with increasing average shear viscosity  $\langle\eta\rangle$ . This shows that a stronger interaction, which leads to a lower shear viscosity, is more efficient in transforming the initial eccentricity to the

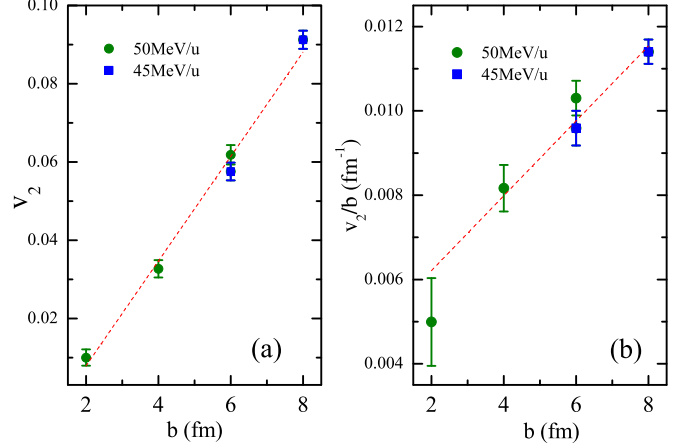


FIG. 3. (Color online) The elliptic flow and that scaled by the impact parameter at balance energies and corresponding impact parameters. Dashed lines are guides for the eye.

final elliptic flow, consistent with the findings in heavy-ion collisions at ultrarelativistic energies. On the other hand,  $v_2/b$  somehow mostly increases with increasing average specific viscosity  $\langle\eta/s\rangle$ , differently from that in ultrarelativistic heavy-ion collisions. This might be due to the stronger dissipation in the hadronic phase than in the partonic phase, which leads to a different behavior of the entropy density in the former case.

In summary, correlations between the impact-parameter-scaled elliptic flow  $v_2/b$  and the shear viscosity  $\eta$  as well as the specific viscosity  $\eta/s$  are investigated based on an IQMD model. Specific combinations of energy and impact parameter, at which directed flow disappears, are selected in  $^{197}\text{Au} + ^{197}\text{Au}$  collisions to remove the blocking effects of the cold spectator matter on the elliptic flow. The shear viscosity is calculated from the parameterized formalism of Danielewicz for the participant nuclear matter, and the local density, temperature, and entropy density are extracted from the hot Thomas-Fermi formalism. Our calculation shows that the scaled elliptic flow from the light fragments with

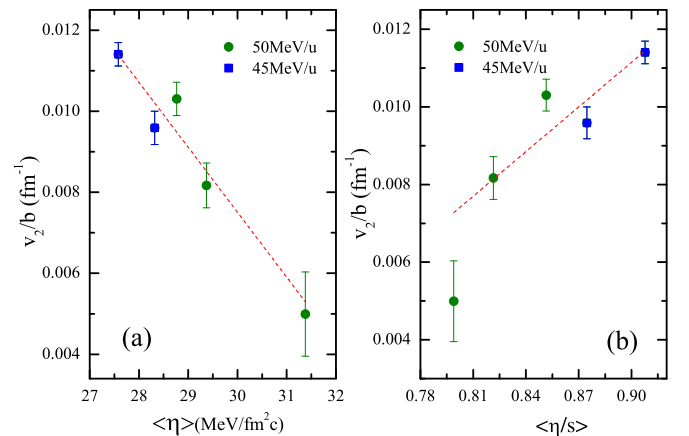


FIG. 4. (Color online) The scaled elliptic flow as a function of the average shear viscosity and specific viscosity at balance energies and corresponding impact parameters. Dashed lines are guides for the eye.

charge number  $Z \leq 3$  drops with increasing shear viscosity, consistent with that observed in ultrarelativistic heavy-ion collisions at the Relativistic Heavy-Ion Collider or Large Hadron Collider. On the other hand,  $v_2/b$  rises with increasing specific viscosity. Our findings are useful for extracting experimentally the shear viscosity and specific viscosity from the elliptic flow in heavy-ion collisions at balance energies.

This work was partially supported by the NSFC under Contract Nos. 11035009, 11220101005, 10979074, 11175231, and 11405248, the Major State Basic Research Development Program in China under Contract Nos. 2014CB845401 and 2013CB834405, the “100-Talent Plan” under Grant No. Y290061011 from the Chinese Academy of Sciences, and the Knowledge Innovation Program of the Chinese Academy of Sciences.

- 
- [1] Y. G. Ma, *Phys. Rev. Lett.* **83**, 3617 (1999); Y. G. Ma *et al.*, *Phys. Rev. C* **71**, 054606 (2005).
- [2] L. G. Moretto, J. B. Elliott, L. Phair, and P. T. Lake, *J. Phys. G* **38**, 113101 (2011).
- [3] J. Adams *et al.* (STAR Collaboration), *Nucl. Phys. A* **757**, 102 (2005).
- [4] R. Lacey *et al.*, *Phys. Rev. Lett.* **98**, 092301 (2007).
- [5] G. Giuliani, H. Zheng, and A. Bonasera, *Prog. Part. Nucl. Phys.* **76**, 116 (2014); H. Zheng, G. Giuliani, and A. Bonasera, *Nucl. Sci. Tech.* **24**, 050512 (2013).
- [6] B. Borderie and M. F. Rivet, *Prog. Part. Nucl. Phys.* **61**, 551 (2008).
- [7] G. Shao *et al.*, *Nucl. Sci. Tech.* **24**, 050523 (2013) ; F. M. Liu, *ibid.* **24**, 050524 (2013) ; C. M. Ko *et al.*, *ibid.* **24**, 050525 (2013).
- [8] C. L. Zhou *et al.*, *Phys. Rev. C* **88**, 024604 (2013).
- [9] C. L. Zhou *et al.*, *Europhys. Lett.* **98**, 66003 (2012).
- [10] S. X. Li, D. Q. Fang, Y. G. Ma, and C. L. Zhou, *Phys. Rev. C* **84**, 024607 (2011).
- [11] D. Q. Fang, Y. G. Ma, and C. L. Zhou, *Phys. Rev. C* **89**, 047601 (2014).
- [12] J. Xu *et al.*, *Phys. Lett. B* **727**, 244 (2013).
- [13] J. Xu, *Nucl. Sci. Tech.* **24**, 050514 (2013).
- [14] L. P. Csernai, J. I. Kapusta, and L. D. McLerran, *Phys. Rev. Lett.* **97**, 152303 (2006).
- [15] P. K. Kovtun, D. T. Son, and A. O. Starinets, *Phys. Rev. Lett.* **94**, 111601 (2005).
- [16] P. Romatschke and U. Romatschke, *Phys. Rev. Lett.* **99**, 172301 (2007).
- [17] H. Song and U. W. Heinz, *Phys. Rev. C* **78**, 024902 (2008).
- [18] P. Huovinen and D. Molnar, *Phys. Rev. C* **79**, 014906 (2009).
- [19] H. Song, S. A. Bass, and U. Heinz, *Phys. Rev. C* **83**, 024912 (2011).
- [20] S. Ryu *et al.*, [arXiv:1210.4588](https://arxiv.org/abs/1210.4588) [hep-ph].
- [21] P. Danielewicz *et al.*, *Science* **298**, 1592 (2002).
- [22] W. Reisdorf *et al.*, *Nucl. Phys. A* **876**, 1 (2012).
- [23] J. Wang *et al.*, *Nucl. Sci. Tech.* **24**, 030501 (2013).
- [24] G. F. Bertsch *et al.*, *Phys. Lett. B* **189**, 384 (1987).
- [25] D. J. Magestro *et al.*, *Phys. Rev. C* **61**, 021602 (2000).
- [26] A. Andronic *et al.*, *Phys. Rev. C* **64**, 041604 (2001).
- [27] Rajni, S. Kumar, and R. K. Puri, *Phys. Rev. C* **84**, 037606 (2011).
- [28] G. Ferini *et al.*, *Phys. Lett. B* **670**, 325 (2009).
- [29] S. A. Voloshin and A. M. Poskanzerr, *Phys. Lett. B* **474**, 27 (2000).
- [30] C. Hartnack *et al.*, *Eur. Phys. J. A* **1**, 151 (1998).
- [31] J. Aichelin, *Phys. Rep.* **202**, 233 (1991).
- [32] C. Hartnack *et al.*, *Nucl. Phys. A* **495**, 303 (1989).
- [33] R. Pak *et al.*, *Phys. Rev. C* **53**, R1469(R) (1996).
- [34] S. Soff, S. A. Bass, C. Hartnack, H. Stöcker, and W. Greiner, *Phys. Rev. C* **51**, 3320 (1995).
- [35] A. D. Sood *et al.*, *Phys. Lett. B* **594**, 260 (2004).
- [36] P. Crochet *et al.*, *Nucl. Phys. A* **624**, 755 (1997).
- [37] W. M. Zhang *et al.*, *Phys. Rev. C* **42**, R491(R) (1990).
- [38] M. D. Partlan *et al.*, *Phys. Rev. Lett.* **75**, 2100 (1995).
- [39] R. Kubo, *Rep. Prog. Phys.* **29**, 255 (1966).
- [40] P. Danielewicz, *Phys. Lett. B* **146**, 168 (1984).
- [41] B. W. Barker and P. Danielewicz, *AIP Conf. Proc.* **1231**, 167 (2010).
- [42] D. T. Khoa *et al.*, *Nucl. Phys. A* **542**, 671 (1992).
- [43] P. K. Puri *et al.*, in *1992 GSI Scientific Report 93-1* (GSI, Darmstadt, Germany), p. 126.
- [44] M. Barranco and J. Treiner, *Nucl. Phys. A* **351**, 269 (1981).
- [45] M. Rashdan *et al.*, *Nucl. Phys. A* **468**, 168 (1987).
- [46] W. K. Wilson *et al.*, *Phys. Rev. C* **41**, R1881(R) (1990).
- [47] M. B. Tsang *et al.*, *Phys. Rev. C* **47**, 2717 (1993).
- [48] R. A. Lacey *et al.*, *Phys. Rev. Lett.* **70**, 1224 (1993).
- [49] W. K. Wilson *et al.*, *Phys. Rev. C* **51**, 3136 (1995).
- [50] Y. G. Ma, W. Q. Shen, J. Feng, and Y. Q. Ma, *Phys. Rev. C* **48**, R1492(R) (1993); Y. G. Ma, W. Q. Shen, and Z. Y. Zhu, *ibid.* **51**, 1029 (1995).
- [51] Y. M. Zheng, C. M. Ko, B. A. Li, and B. Zhang, *Phys. Rev. Lett.* **83**, 2534 (1999).